PHASE INTERACTION AND DISTRIBUTION IN MIXED IONIC ELECTRONIC CONDUCTING CERIA-SPINEL COMPOSITES

M. Ramasamy[a], S. Baumann[a], A. Opitz[b,e], R. Iskandar[c], J. Mayer[c], D. Udomsilp[a,e] U. Breuer[d], M. Bram[a,e]
[a]Forschungszentrum Jülich GmbH, Insitute of Energy and Climate Research IEK-1, 52425 Jülich, DE
[b]Vienna University of Technology, Institute of Chemical Technologies and Analytics, 1060 Wien, AT
[c]RWTH Aachen University, Gemeinschaftslabor für Elektronenmikroskopie (GFE), 52074 Aachen, DE
[d]Forschungszentrum Jülich GmbH, Central Institute of Engineering Electronics and Engineering ZEA-3, 52425 Jülich, DE
[e]Christian Doppler Laboratory for Interfaces in Metal-Supported Electrochemical Energy Converters

ABSTRACT

Mixed Ionic electronic conductors find various applications as SOFC cathodes and oxygen transport membranes. Dual phase composites are a promising class of thermochemical stable materials, in which two ceramic phases are coupled to provide a pure electronic and ionic conducting pathway, respectively. Composites of 20 mol% Gadolinia doped ceria (GDC) and $FeCo_2O_4$ spinel (FCO) are investigated. GDC-FCO 60:40 wt-% ratio showed reasonable oxygen permeation with ionic conductivity as the limiting factor. Spinel content was reduced to as low as 10 wt-% in the composite and their corresponding electrical conductivity and oxygen permeation were measured from which ambipolar conductivity was calculated. GDC-FCO 85:15 wt-% ratio shows the highest ambipolar conductivity comparable to standard single phase $La_{0.58}Sr_{0.4}Fe_{0.8}Co_{0.2}O_{3-\delta}$ (LSCF) at 850 °C. The Microstructure analysis showed reversible and thus temporary spinel decomposition at sintering temperature as well as phase interaction forming a Gd- and Fe-rich orthorhombic perovskite with traces of Ce and Co. To further investigate the phase interaction and secondary phase formation, Pulsed Layer Deposition of FCO layer (~400 nm) on a polycrystalline GDC substrate and annealing at varying temperatures and times from 1000 to 1200 °C were carried out. These samples were analyzed by XRD, STEM, and SIMS to understand the interlayer interaction of the phases.

INTRODUCTION

MIEC Oxygen transport membranes contribute to major research focus in the last two decades due to its ability to separate pure oxygen from air more efficiently compared to other technologies[1]. Recently, increasing research interest is drawn to the development of membrane reactors, combining the separation task with a catalytically promoted chemical reaction. Such process intensification is interesting in different fields such as energy applications as well as the production of fine chemicals[2, 3, 4, 5].

In particular Ceria based MIEC are also attractive in Hydrocarbon fuel utilization due to their resistance to reducing atmospheres as well as carbon deposition [1, 6]. Ceria based Fluorites combined with transition metal oxides with spinel structure have proven to improve the sinter ability and mixed conductivity of the composite [7, 8, 9]. Moreover, dual phase composites like GDC-LSCF have been studied as potential SOFC cathode layer [10, 11, 12]. Particularly for metal supported SOFCs there is a need in cathode material development, which can be sintered in relatively low p_{O2} in order to prevent catastrophic metal support oxidation. However, standard materials such as $La_{0.58}Sr_{0.4}Fe_{0.8}Co_{0.2}O_{3-\delta}$ (LSCF) do not withstand such conditions. Hence, the development of composite materials with good reduction stability is of great importance.

In this paper, various ratio combinations of GDC ($Ce_{0.8}Gd_{0.2}O_{2-\delta}$) and FCO ($FeCo_2O_4$) were synthesized, and their dense pellets were studied for their mixed conductivity by measuring their oxygen flux performance at high temperatures. The work also focuses on the phase interaction and secondary phase formation of the composite to better understand the conductivity behavior of the composites. This work indicates the possibility of highest oxygen transport in

this dual phase membrane with electronic conducting phase as low as 18.5 vol%. In addition, this composite was tested for its cathodic activity for application in SOFC.

EXPERIMENTAL

GDC-FCO composites of ratios varying spinel content from 46 vol% to as low as 12.5 vol % be synthesized by modified Pechini process. The powders were calcined at 700°C for 15h to attain the desired fluorite and spinel phases. The different ratio composite powders were pressed into cylindrical pellets of 20mm dia by uniaxial pressing at 80 Mpa for 90 seconds. The pellets were sintered at 1200°C for 10h to obtain dense pellets with relative theoretical density of ~97 %, which were also tested for gas tightness by Helium leak test using Pfeiffer vacuum apparatus. Electrical conductivity of bars was measured by DC four point conductivity between temperatures 600 to 850°C. Thin layers of FCO were deposited on polycrystalline GDC substrates by means of pulsed laser deposition (PLD). FCO target was ablated by a KrF excimer laser (248 nm; 5 Hz repeat rate). The substrate temperature was 650°C (controlled by a pyrometer), background pressure of pure oxygen in the chamber was $4x10^{-2}$ mbar, and deposition times were ca. 25 min to obtain a film thickness of about 100 nm.

X-ray diffraction (XRD) analysis of the dual phase compounds was performed on D4 Endeavor (Bruker AVS) with CuKα radiation measured at $10° \leq 2\theta \geq 80°$, $\Delta 2\theta = 0.02°$. X-ray diffraction analysis of FCO thin films was carried out on a PANalytical Empyrean diffractometer with CuKα radiation. Thin film XRD measurements were conducted with 2° incident angle and diffraction pattern was recorded at $15° \leq 2\theta \geq 90°$. Data analysis was performed with the software Highscore Plus in combination with ICDD powder diffraction database (PDF4+)[13]. Phase identification and microstructure analysis of the dense pellets were carried out using SEM (Zeiss Ultra55). The Scanning transmission electron microscopy (STEM) images were acquired using Zeiss Libra 200FE equipped with a cold FEG source operated at 200 KV, HAADF detector from Fischione and X-Flash EDS detector from Bruker. ESPRIT software was used to analyze and build the EDS elemental maps. SIMS investigation was carried out using TOF-SIMS 4 (IonTOF, Germany) with Cs ion beam for sputtering (2 KeV) and Bi1gun (25KeV) for analysis.

The dense disk type pellets polished to a thickness of 1mm each were measured for their oxygen flux using the quartz permeation setup at IEK-1 in the temperature range of 600 to 1000°C. Air and argon were used as the feed and sweep gas at the flow rate of 250 ml/min to 50ml/min, golden rings used to seal the sample in the setup. Samples were screen printed with catalytic LSCF layer on both sides and post sintered at 1050 °C for 3 h[7].

Symmetrical cells of 10 x 10 mm² were prepared by screen printing of GDC-FCO (85:15) slurry on both sides of 200 µm thick 8YSZ substrates (Kerafol, Germany) and subsequent sintering at 1080 °C for 3 h in ambient air. As a contact layer ca. 300 nm Au were sputter deposited on both sides of these symmetrical samples. The polarization resistance of the electrodes was tested at temperatures between 600 and 900 °C by electrochemical impedance spectroscopy (EIS) in order to estimate the suitability of GDC-FCO composites as SOFC dual phase cathode material. . Measurements were conducted on a PSM 1735 machine with 4 point impedance analysis interface (both: N4L, UK); AC voltage was set to 20 mV root-mean-square; measured frequency range was between 10 mHz and 100 kHz.

RESULTS AND DISCUSSION

In the previous work, we investigated Fluorite-Spinel composite for oxygen transport membrane by combining 60 wt % of GDC ($Ce_{0.8}Gd_{0.2}O_{2-x}$) with 40 wt % of FCO ($FeCo_2O_4$) (54 vol% GDC – 46 vol% FCO) in comparison to standard perovskite material LSCF. The detailed investigation of the dual phase membrane revealed phase interaction and secondary phase formation during the sintering process i.e $GdFeO_3$ perovskite with traces of Ce and Co formed by

the interdiffusion during sintering at 1200°C. Inspite of this additional phase, Permeation tests resulted in reasonable oxygen flux, when slow surface exchange was facilitated by catalytic active porous coatings[7]. Thus with elimination of surface exchange limitation , the activation energy of bulk diffusion over the whole temperature range of 650° C-1000°C was 66 kJ/mol[7]. This clearly indicates that the ionic conductivity is the limiting step in the bulk transport as it matches the activation energy of pure GDC corresponding to its bulk ionic transport for the same temperature range. Therefore, an increase in the GDC-content would be beneficial. On the other hand, the proportion of both phases in a dual phase composite must be high enough to form continuous phases in the bulk and surfaces, i.e. both phases need to reach a state of percolation. To reach the percolation threshold, the volume fraction of the minor phase is usually no less than 30% for dual-phase materials[14]. Nevertheless this is not necessarily applicable for composites that tend to have phase interaction and grain boundary phases. The grain boundary phase and secondary phases formed are possibly conducting, contributing to the overall percolating network of the composite impacting the oxygen transport. Hence, the spinel content is reduced from 40 wt% to as low as 10 wt% in the composite as shown in Table I for this investigation and powders were synthesized by the one pot Pechini process.

Table I Composites with reducing spinel content given in Weight % and Volume %

GDC-FCO ratios in wt %	GDC-FCO ratios in Vol %
60:40	54:46
65:35	59:41
70:30	64.5:35.5
75:25	70:30
80:20	76:24
85:15	81.5:18.5
90:10	87.5:12.5

Microstructure analysis

The XRD plots of the composites with varying spinel content are shown in Figure 1. The decrease in spinel content is evident from the decrease in intensity of the spinel peaks of the composites particularly at 31° and 64° 2θ. In addition, the presences of orthorhombic perovskite peaks (between 24° and 33° 2θ) are confirmed in all the ratios. These results are further supported by the SEM images as shown in Figure 2. The images show the presence of fluorite phase with decreasing distribution of the spinel phase corresponding to the ratio and the presence of orthorhombic perovskite phase in all the four cases [7, 15]. Going into in-depth investigation of the microstructure by STEM analysis of the lowest spinel content ratio composite 90:10 GDC-FCO, it is evident that the third phase $GdFeO_3$ (orthorhombic perovskite) contains traces of Ce and Co elements as well. STEM-HAADF and EDS element mapping of 90:10 ratio composite is shown in Figure 3. Semi quantitative estimation of the elements from the EDS elemental mapping image provides a hint on the approximate composition of the perovskite phase that is formed in these dual phase composites during the sintering process i.e., 15%Ce on A-site, 25% Co on B-site in $GdFeO_3$ perovskite phase. The $Gd_{0.85}Ce_{0.15}Fe_{0.75}Co_{0.25}O_3$ (GCFCO) phase is also observed to be individual grains with no obvious grain boundary phase visible in this magnification. Thus it would be worthwhile to investigate this perovskite phase for its transport behavior to identify its role in the composite for oxygen permeation.

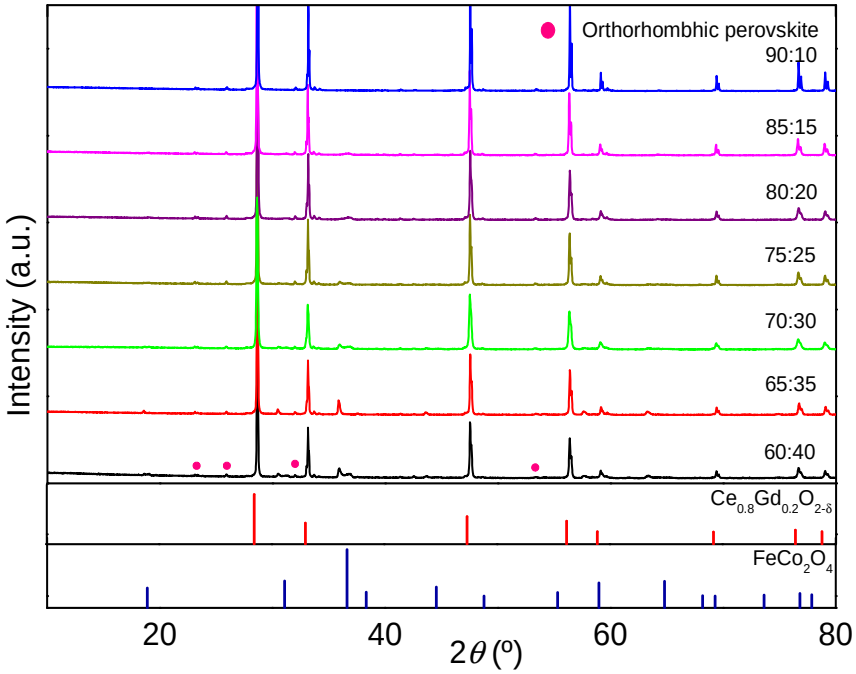

Figure 1 XRD plots of the composites with varying spinel content from 40 wt% to 10 wt% sintered at 1200°C for 10h

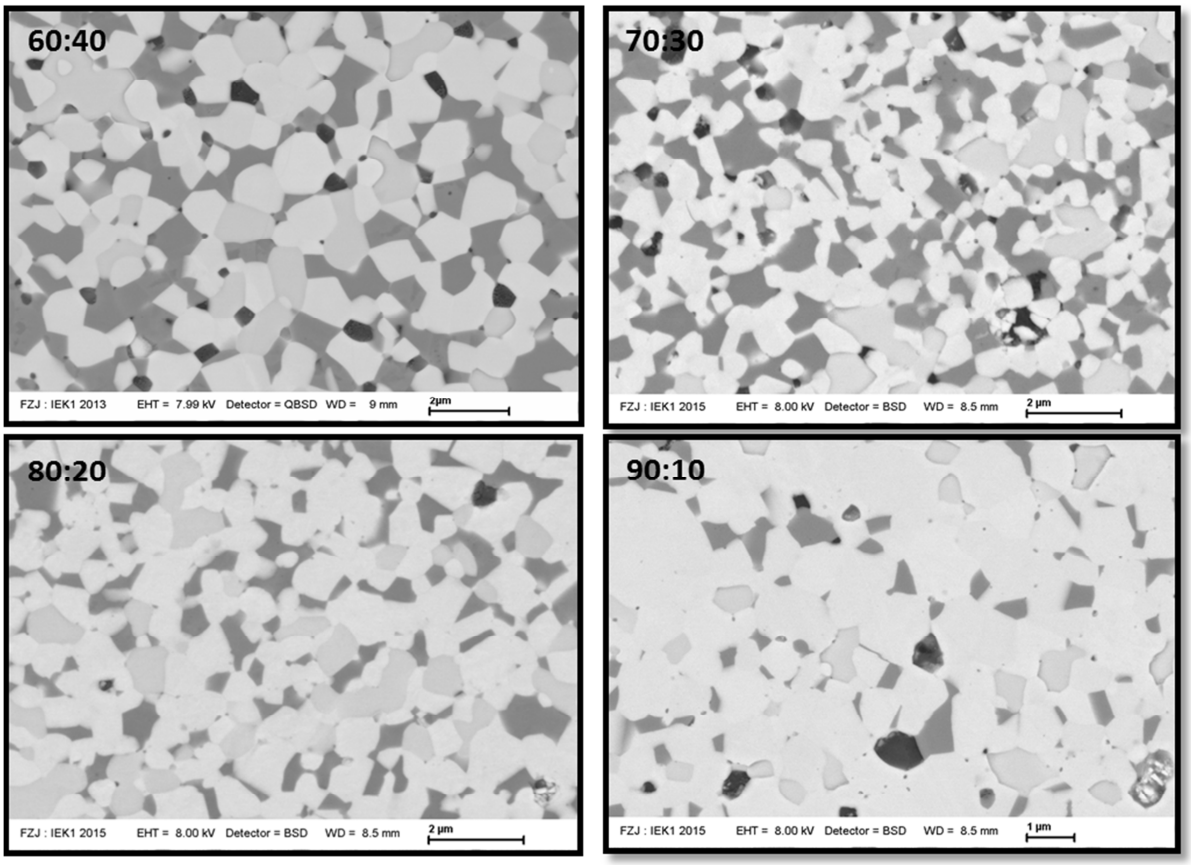

Figure 2 SEM images of GDC-FCO composites with ratios 60:40 (top left), 70:30 (top right), 80:20 (bottom left) and 90:10 (bottom right).

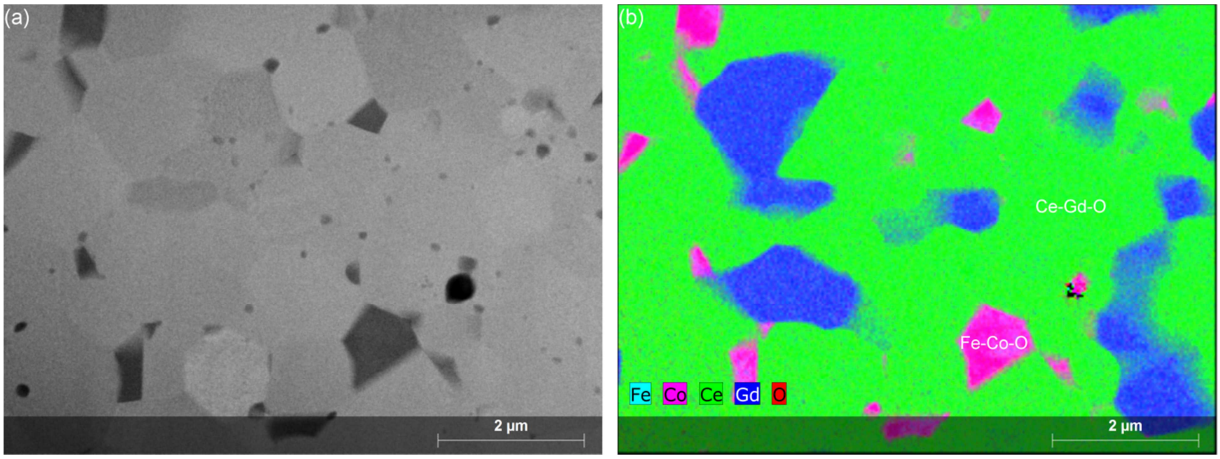

Figure 3 STEM-HAADF and EDS element mapping of GDC-FCO 90:10 ratio composite sintered at 1200°C for 10h

Electrical Conductivity

Bars of all the composite ratios and their corresponding individual phases were fabricated and subjected total conductivity measurements by four point DC method. The electrical conductivity results of GDC-FCO ratios are compared to standard composition 60: 40 GDC-FCO ratio, pure GDC, FCO and GCFCO (composition semi quantified from EDS elemental mapping). Figure 4 shows the compiled results of all the varying ratio dual phase composites and the individual phases constituing the composite for direct comparison. The electrical conductivity of FCO being the higest as expected followed by decreasing spinel content indicating that the electronic conductivity is still dominant.

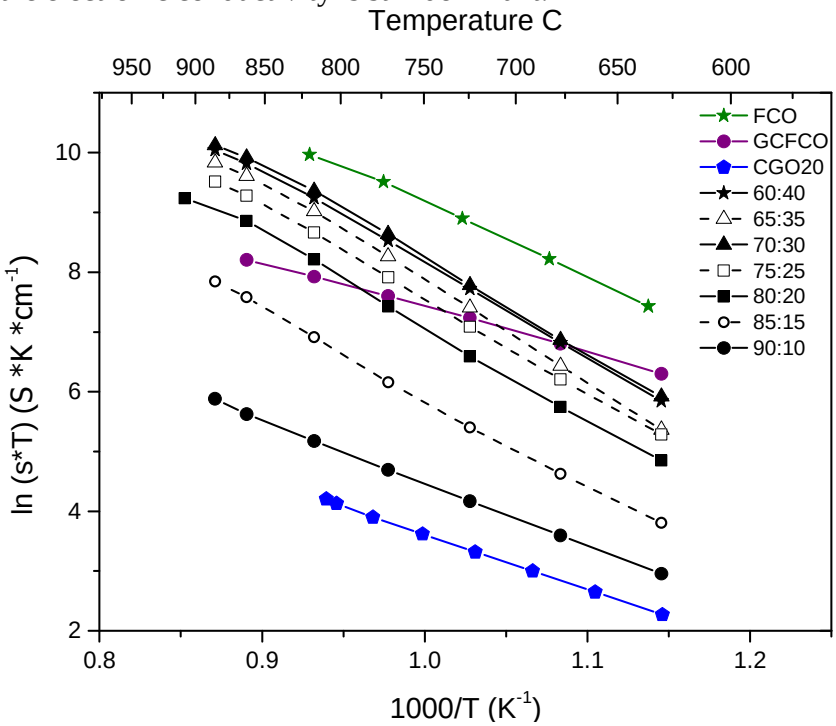

Figure 4 Electrical conductivities of GDC-FCO composites with varying spinel content from 40 wt% to 10 wt% by four point DC method.

The conductivity decreases consistently with the spinel content decreased upto 10 wt%. Interestingly the 90:10 ratio sample still shows higher electrical conductivity than pure GDC. This signifies the presence of a percolating network of electronic conductor even with as low as

10 wt% of spinel content. The GCFCO phase shows relatively high electrical conductivity than pure GDC but lower than pure FCO signifying its non-hinderance to the oxygen flux when present in the dual phase composite and might be categorized as a MIEC phase contributing to the oxygen transport. In our previous work, investigation of pure $GdFeO_3$ as indivivdual phase indicated negligable electrical conductivity. But this semi quantitative estimated perovksite phase with traces of Ce and Co in the structure are the possible promoters of the conducitivty which in turn impacts the flux as well [16, 17].

Permeation measurements

The composites with the varying spinel content were subjected to permeation measurements between 700° to 1000°C temperatures with Air and Argon as the feed and sweep gas respectively. Catalytic porous layer coating of LSCF over all the composite ratios was applied to eliminate surface exchange limitations which was evident in the standard composite reported in our previous work.

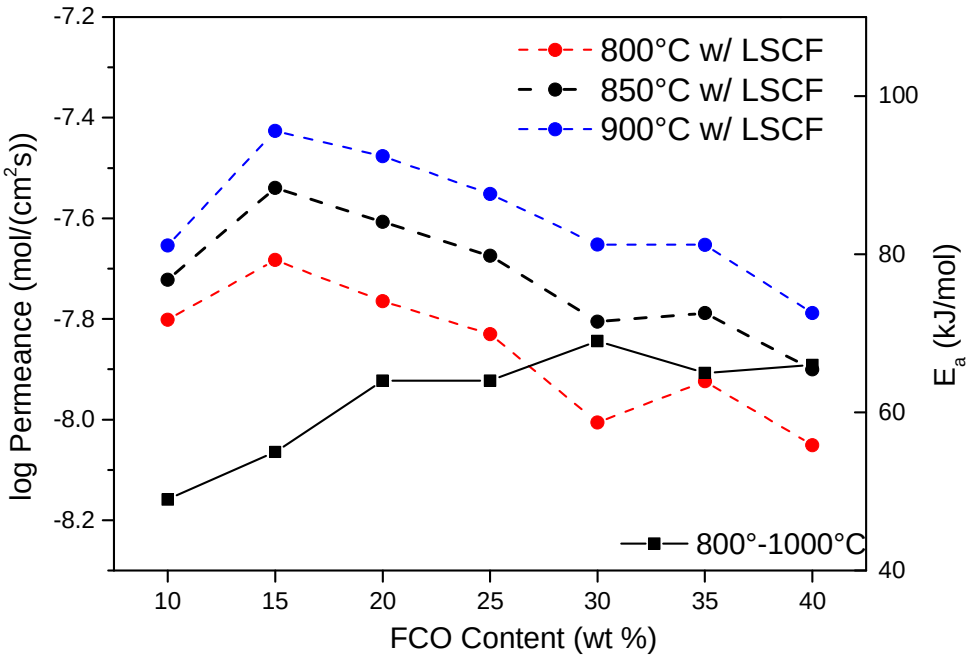

Figure 5 Plot as a function of permeance for varying spinel content in the GDC-FCO composite and their corresponding calculated activation energy between 800°-1000°C

The permeance of the samples are calculated normalizing the partial pressure gradient which are plotted against the varying spinel content for temperatures 800°C, 850°C and 900°C. Activation energy E_a for each sample is also calculated from the measured oxygen flux plotted in the same graph as shown in Figure 5. The oxygen permeance of the composites show steady increase with decreasing spinel content eventually attaining the highest permeance value for 15 wt% spinel content composite. The permeance value drops down for 10 wt% spinel sample indicating the lack of necessary percolating network for efficient oxygen transport. On the other hand, activation energy maintains its constantcy with decerasing spinel content upto 20 wt% spinel ratio but begins to drop with further reduced spinel content. From 40 to 20 wt% of spinel in the composite, the E_a is constant at approx 66 kJ/mol indicating that the ionic conductivity of GDC is the rate limiting step [7]. Below 20 wt% spinel phase the activation energy decreases indicating a change in the limiting transport process, probably electronic conductivity.

Summarizing the permeance and activation energy results , it can be stated that electronic conductivity becomes the limiting factor in the composites possessing less than 20 wt % spinel

content. 85:15 ratio proves to be the highest oxygen transporting membranes among the investigated compositions. Thus 15 wt% spinel content can be regarded as the appropriate proportion at which the limiting process is changing, but still with significant percolating network of electronic conductance that provides highest oxygen flux. From the electrical conductivity of GCFCO phase, it is evident that there are no hinderance to the oxygen transport and might be categorized as a MIEC phase present in the composite. Nonetheless, the ambipolar conductivity calculated from the permeation measurement of GCFCO is negligable categorizing it as a pure electronic conductor with no siginifcant ionic transport. Thus, it is clear that GDC-FCO 85:15 ratio shows significant oxygen transport with 85 wt% GDC contributing to the ionic transport, while GCFCO and FCO phases are responsible for electronic transport altogether forming the efficient percolating network of the membrane.

Phase interaction study

In order to investigate the phase interaction noticed in the composite with more depth, a systematic study was performed. Polished GDC pellets were PLD coated with FCO and subsequently subjected to different annealing temperatures for varying dwell times to investigate the phase interaction and hence the formation of the orthorhombic perovskite phase.

Table II Annealing temperatures and dwell times

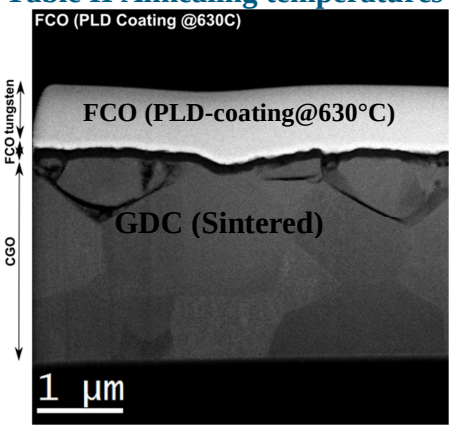

Time h	Temperature °C			
	1000	1050	1100	1200
	1	3	1	1
	3	6		5
	5			10
	15			
	45			

Figure 6 STEM-HAADF image of a GDC substrate PLD coated with FCO layer as deposited

XRD measurements were done in a mode with 2° incident angle yielding less intensity from the substrate and more intensity from the thin film. Directly after PLD-deposition , the samples show patterns of GDC, as well as two spinels – nominally $CoCo_2O_4$ and Fe_2CoO_4. Taking into account the sintering temperature of the composites investigated above, samples were first annealed at 1200°C for various times as mentioned in the Table II. The X-ray diffractograms clearly show that already after 1 hour all of the spinel phase disappears and only two main phases – GDC and $Gd(Fe,Co)O_3$-perovskite are present. In case of lower annealing temperatures (Figure 7), the onset of $Gd(Fe,Co)O_3$-perovskite phase in XRD pattern seems to occur at different dwell times such as a) at 1100°C after 1 hour, b) 1050°C for 3h and c) 1000°C for 15h. The three main phases – GDC, $CoCo_2O_4$-spinel, and $Gd(Fe,Co)O_3$-perovskite are observed. In case of the EDS mapping in STEM as shown in Figure 8, the onset of phase interaction can already be observed after 3h of annealing time at 1000°C. (Please note: Absent perovskite signals in the XRD pattern of samples beeing annealed shorter than 45h can most likely be explained by the low incident angle in XRD leading to lower sensitivity for signals from phases at the film-substrate interface.)

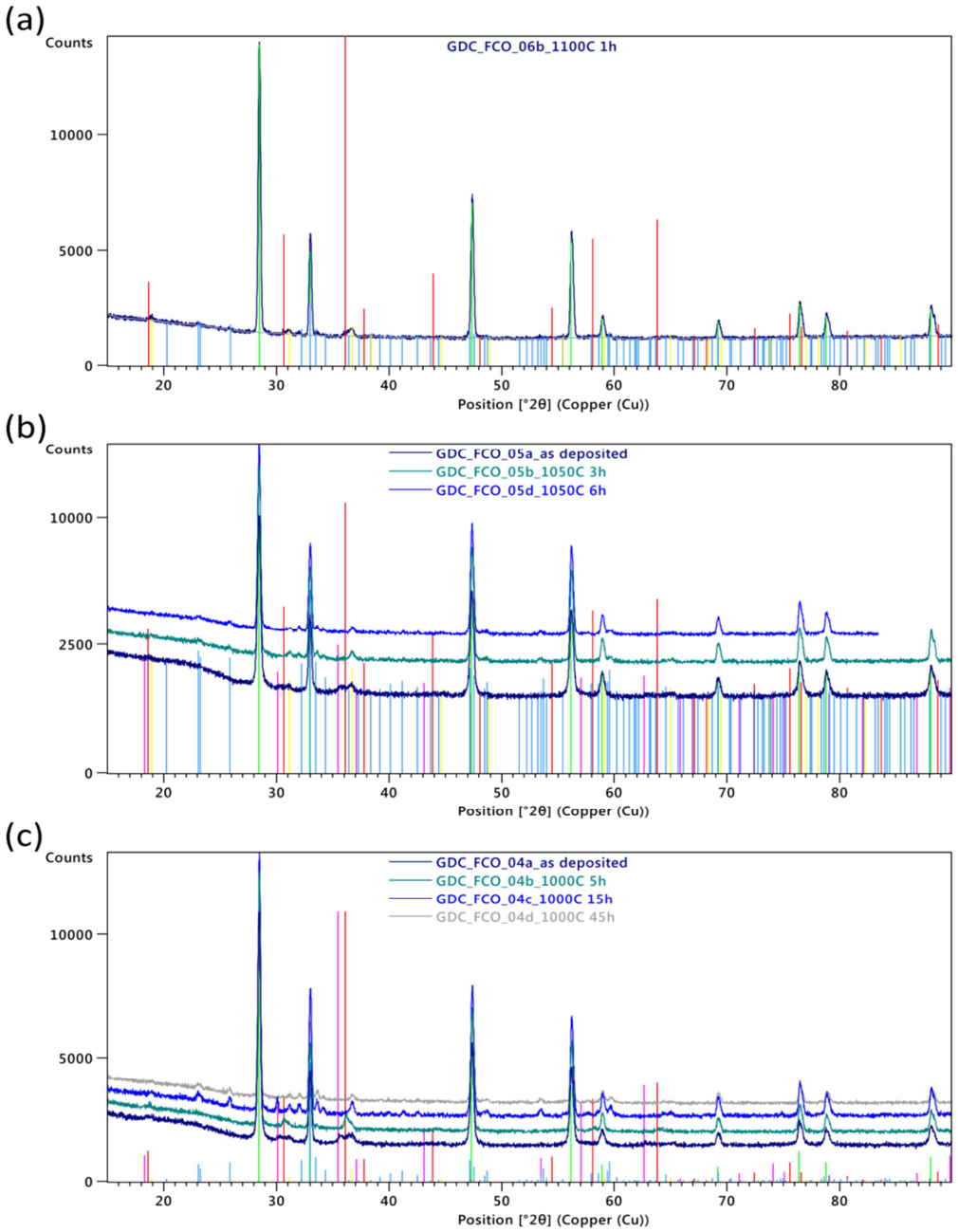

Figure 7 Diffraction pattern measured on thin film samples after annealing at (a) 1100 °C (b) 1050 °C and (c) 1000 °C. The vertical lines indicate literature pattern from PDF database: GDC (green), $FeCo_2O_4$ (red), Fe_2CoO_4 (pink), $CoCo_2O_4$ (yellow), $Gd(Fe,Co)O_3$ (light blue)

Figure 8(top) depicts the broader area of the sample with few grains of spinel and perovskite phase non-homogenously distributed over the GDC substrate. This scarce distribution could attribute to contraction of the spinel layer associated with high reactivity of Fe cations with Gd in comparison to the Co cations at the annealing temperature. While Figure 8(bottom) looks into one particular grain marked as A1 at higher magnification and the EDS mapping confirms the presence of Gd and Fe rich perovskite with traces of ce and Co adjacent to Fe_2CoO_4 spinel phase. Also due to non-uniformity of the coating thickness, the intensity of interaction may vary from sample to sample as observed by the STEM analysis.

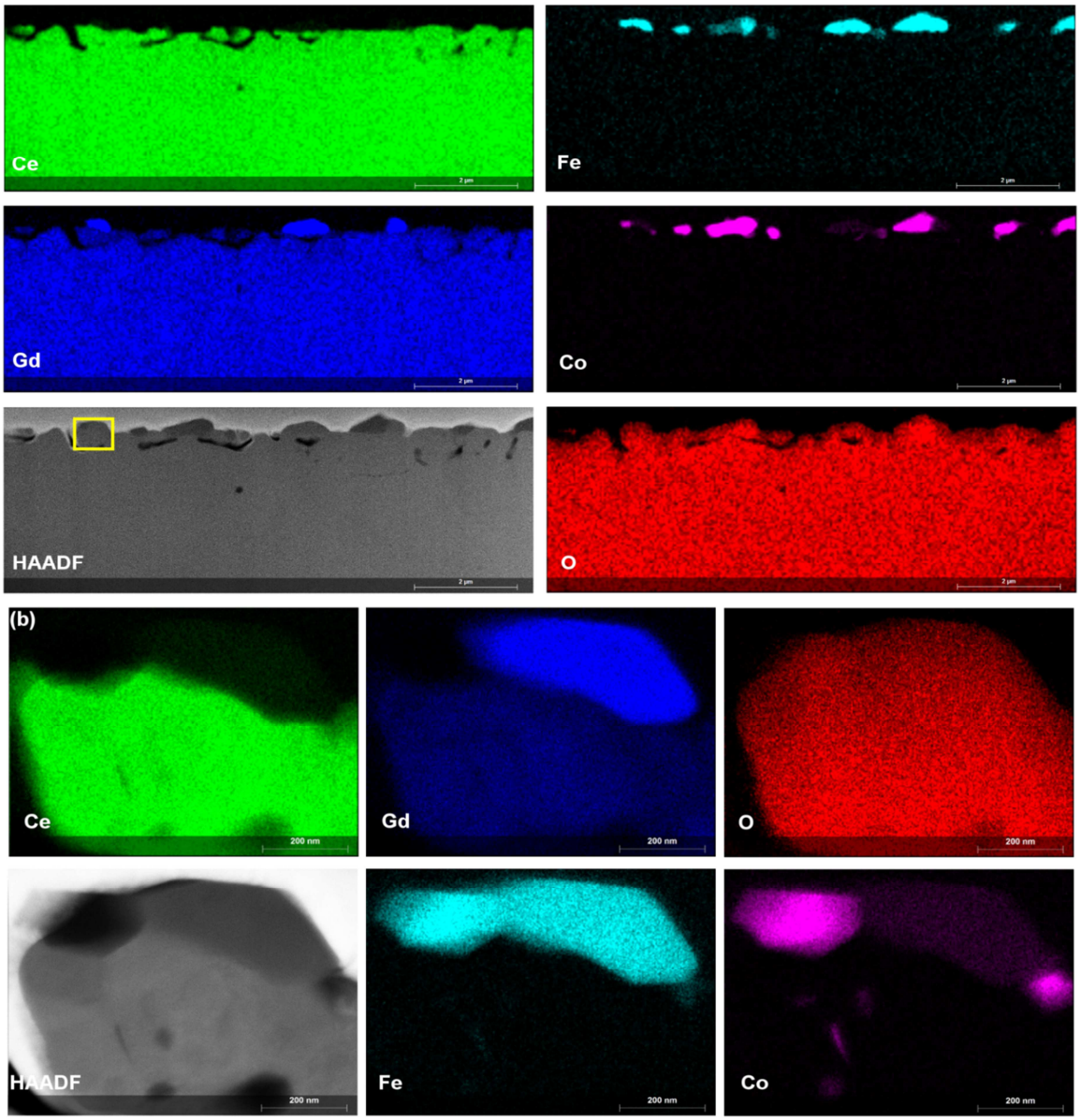

Figure 8 EDS net count mapping of the 1000°C 3h(top) and higher magnification EDS mapping of A1(bottom) marked in image on the left.

Thus the Fe containing spinel seems to be more reactive in terms of forming a perovskite phase with Gd from the GDC, whereas the Co-rich spinel seems to be more stable. At elevated temperature obviously the Fe is preferentially removed from the spinel phase(s) leaving behind the Co-rich spinel phase.

Based on the XRD and STEM results it is evident that the perovskite is formed at 1000°C and above temperatures, while the distribution of phases depends on the dwell time to a certain extent. Hence for investigation by SIMS (Secondary Ion Mass spectrometry) analysis samples annealed at 1050°C for 6h and its as deposited counterpart were chosen as shown in Figure 9.

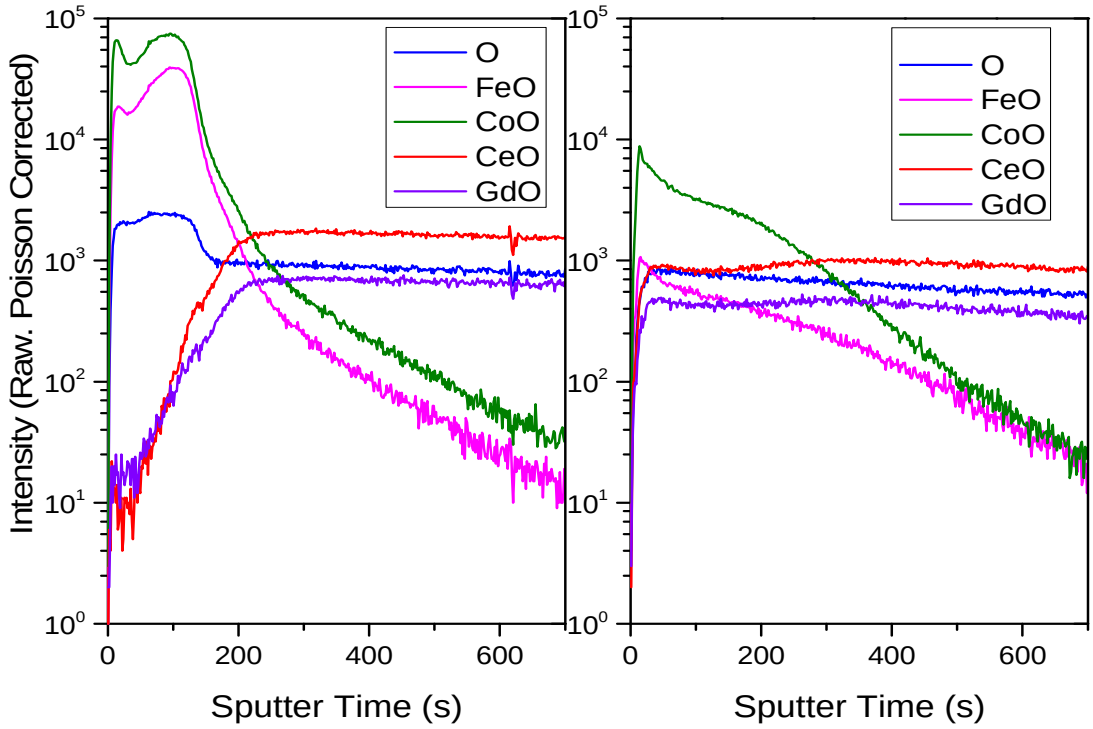

Figure 9 SIMS plot of as deposited (left) and 1050°C 6h annealed (right) samples.

The profiling of both the samples to a penetration depth of 70 µm was carried out to observe the phase transition. The as deposited sample clearly separates the spinel phase by the FeO and CoO high intensity profiles dominating for a certain depth followed by CeO and GdO profiles representing the flourite phase for the remaining depth of the analysis. However the annealed sample shows high intensity CoO profile for a certain depth, whereas the FeO profile is much lesser intensity proving its higher diffusivity in this material system. Moreover, GdO and CeO profiles now are present upto the surface of the sample. The results supports the former results leading to the conclusion that Fe is preferably extracted from the spinel phase forming a new perovskite phase rich in Gd and Fe with traces of Ce and Co. The remaining spinel phase in consequence is rich in Co.

GDC-FCO cathode testing

Preliminary impedance results measured on symmetrical cells (10 x 10 mm² 85:15 composite of GDC-FCO on both sides of 8YSZ substrate) are shown in Figure 10. All spectra consist of a rather uncommon high frequency feature and a relatively unsymmetric low frequency arc. The latter appears to contain at least two different contributions whereas the high frequency part may be an artifact resulting from the contacting of the sample and the relatively poor in plane conductivity of the electrodes. A more detailed analysis of impedance data is, however, not possible from the data available so far. Though, an estimation of the electrodes polarization resistance is still possible from these impdance spectra. In measurements with symmetrically extended metal electrodes the 8YSZ substrates showed about 0.4 – 0.5 Ω of ohmic resistance at 800 °C. The measured total resistance of the FCO-GDC electrodes at this temperature is ca. 1.5 Ω (see Figure 10), From these values an area specific resistance (ASR) of ca. 0.5 – 0.6 Ωcm² can be estimated.

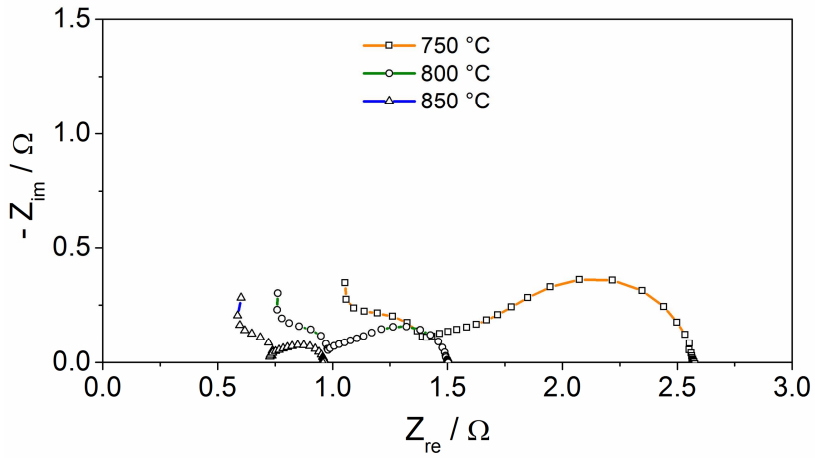

Figure 10 Impedance spectra (Nyquist plot) of a sample with symmetrical GDC-FCO dual phase cathode measured at three different temperatures.

This value is considerably higher compared to state-of-the-art LSCF cathodes that exhibit ASRs lower than 0.1 Ωcm² at 800 °C [12] and ASRs of single cells of about 0.2 Ωcm² [11]. Nevertheless, these results are promising because there is still a lot of potential improvement possible via optimization of both material's composition as well as layer's microstructure. Since in-plane conductivity of the electrodes was rather poor, the low electronic conductivity may be responsible for a large part of the measured polarization resistance. Therefore, increasing FCO content should improve the cathode performance in contrast to the use as oxygen transport membrane. Further experiments with varying GDC-FCO composition for SOFC operation are necessary in order to find its optimum as cathode material. Moreover, microstructure optimization has to be done in order to maximize the catalytically active triple phase boundaries (TPB) and, hence, minimize the observed surface exchange limitation.

CONCLUSIONS

Dual phase composite GDC-FCO with varying spinel content show corresponding electrical conductvity in the order of spinel content present in the composite. GDC-FCO 85:15 ratio content proves to be excellent oxygen transport membrane with highest oxygen flux. The phase interaction between spinel and flourite phases to form the perovskite phase is investigated in depth by PLD coating a thin film of FCO over GDC substrate and characterised using XRD, STEM and TOF-SIMS. The FCO film after annealing at 1000°C for over 3h show phase transition as Fe tends to be more reactive with Gd to form the perovskite phase leaving behind a Co-rich spinel phase.

Due to its high mixed conductivity , the composite was tested for its suitability as a potential cathode layer for SOFCs. EIS measurements of symmetrical cells (GDC-FCO/8YSZ/GDC-FCO) confirmed catalytic activity regarding reduction of oxygen and incorporation of the oxygen ions, resulting in an ASR of 0.6 Ωcm². Increased performance as SOFC cathode is expected by optimization of composition and microstructure, since the initial experiments were based on the composite optimized for the use as oxygen transport membrane.

ACKNOWLEDGEMENTS

The work is financially supported by the European Commission via the FP7 project GREEN-CC (Grant Agreement no. 608524), The German Bundesministerium für Bildung und Forschung (BMBF) Funding No: 03EK3032, and Christian Doppler Laboratories funded by the Austrian Bundesministerium für Wissenschaft, Forschung und Wirtschaft (BMWFW). The X-

ray center of the TU Wien is gratefully acknowledged for assistance with XRD measurements and provision of data analysis software.

REFERENCES

[1] J. Sunarso, S. Baumann, J. M. Serra, W. A. Meulenberg, S. Liu, Y. S. Lin, and J. C. Diniz da Costa, "Mixed ionic–electronic conducting (MIEC) ceramic-based membranes for oxygen separation," *Journal of Membrane Science,* 320[1–2] 13-41 (2008).

[2] Z. Cao, H. Jiang, H. Luo, S. Baumann, W. A. Meulenberg, H. Voss, and J. Caro, "An Efficient Oxygen Activation Route for Improved Ammonia Oxidation through an Oxygen-Permeable Catalytic Membrane," *ChemCatChem,* 6[5] 1190-94 (2014).

[3] Z. Cao, H. Jiang, H. Luo, S. Baumann, W. A. Meulenberg, J. Assmann, L. Mleczko, Y. Liu, and J. Caro, "Natural Gas to Fuels and Chemicals: Improved Methane Aromatization in an Oxygen-Permeable Membrane Reactor," *Angewandte Chemie International Edition,* 52[51] 13794-97 (2013).

[4] Y. Wei, W. Yang, J. Caro, and H. Wang, "Dense ceramic oxygen permeable membranes and catalytic membrane reactors," *Chemical Engineering Journal,* 220 185-203 (2013).

[5] X. Dong, W. Jin, N. Xu, and K. Li, "Dense ceramic catalytic membranes and membrane reactors for energy and environmental applications," *Chemical Communications,* 47[39] 10886-902 (2011).

[6] M. Mogensen, N. M. Sammes, and G. A. Tompsett, "Physical, chemical and electrochemical properties of pure and doped ceria," *Solid State Ionics,* 129[1–4] 63-94 (2000).

[7] M. Ramasamy, S. Baumann, J. Palisaitis, F. Schulze-Küppers, M. Balaguer, D. Kim, W. A. Meulenberg, J. Mayer, R. Bhave, O. Guillon, and M. Bram, "Influence of Microstructure and Surface Activation of Dual-Phase Membrane Ce0.8Gd0.2O2−δ–FeCo2O4 on Oxygen Permeation," *Journal of the American Ceramic Society* 10.1111/jace.13938 (2015).

[8] M. Balaguer, V. B. Vert, L. Navarrete, and J. M. Serra, "SOFC composite cathodes based on LSM and co-doped cerias (Ce0.8Gd0.1X0.1O2–δ, X = Gd, Cr, Mg, Bi, Ce)," *Journal of Power Sources,* 223[0] 214-20 (2013).

[9] S. B. Adler, "Factors Governing Oxygen Reduction in Solid Oxide Fuel Cell Cathodes†," *Chemical Reviews,* 104[10] 4791-844 (2004).

[10] Y. Leng, S. H. Chan, and Q. Liu, "Development of LSCF–GDC composite cathodes for low-temperature solid oxide fuel cells with thin film GDC electrolyte," *International Journal of Hydrogen Energy,* 33[14] 3808-17 (2008).

[11] A. Mai, V. A. C. Haanappel, S. Uhlenbruck, F. Tietz, and D. Stöver, "Ferrite-based perovskites as cathode materials for anode-supported solid oxide fuel cells: Part I. Variation of composition," *Solid State Ionics,* 176[15–16] 1341-50 (2005).

[12] E. Perry Murray, M. J. Sever, and S. A. Barnett, "Electrochemical performance of (La,Sr)(Co,Fe)O3–(Ce,Gd)O3 composite cathodes," *Solid State Ionics,* 148[1–2] 27-34 (2002).

[13] S. Kabekkodu, " ICDD PDF-4+ Database, In: International Centre for Diffraction Data." in. Editor, Newtown Square, PA, USA, 2010.

[14] X. Zhu, H. Wang, and W. Yang, "Relationship between homogeneity and oxygen permeability of composite membranes," *Journal of Membrane Science,* 309[1–2] 120-27 (2008).

[15] Y. Lin, S. Fang, D. Su, K. S. Brinkman, and F. Chen, "Enhancing grain boundary ionic conductivity in mixed ionic-electronic conductors," *Nat Commun,* 6 (2015).

[16] M. Sun, X. Chen, and L. Hong, "Influence of the interfacial phase on the structural integrity and oxygen permeability of a dual-phase membrane," *ACS Applied Materials and Interfaces,* 5[18] 9067-74 (2013).

[17] J. Zhou, X. Tang, D. He, C. Wu, Y. Zhang, W. Ding, Y. Jin, and C. Sun, "Oxygen permeability and CO2-tolerance of Ce0.9Gd0.1O2−δ – SrCo0.8Fe0.1Nb0.1O3−δ dual-phase membrane," *Journal of Alloys and Compounds,* 646 204-10 (2015).